Viewpoint-independent Single-view 3D Object Reconstruction using Reinforcement Learning

Seiya Ito[a], Byeongjun Ju, Naoshi Kaneko[b] and Kazuhiko Sumi[c]
Department of Integrated Information Technology, Aoyama Gakuin University, Fuchinobe, Sagamihara, Japan

Keywords: 3D Object Reconstruction, Reinforcement Learning.

Abstract: This paper addresses the problem of reconstructing 3D object shapes from single-view images using reinforcement learning. Reinforcement learning allows us to interpret the reconstruction process of a 3D object by visualizing sequentially selected actions. However, the conventional method used a single fixed viewpoint and was not validated with an arbitrary viewpoint. To handle images from arbitrary viewpoints, we propose a reinforcement learning framework that introduces an encoder to extract viewpoint-independent image features. We train an encoder-decoder network to disentangle shape and viewpoint features from the image. The parameters of the encoder part of the network are fixed, and the encoder is incorporated into the reinforcement learning framework as an image feature extractor. Since the encoder learns to extract viewpoint-independent features from images of arbitrary viewpoints, only images of a single viewpoint are needed for reinforcement learning. The experimental results show that the proposed method can learn faster and achieves better accuracy than the conventional method.

1 INTRODUCTION

Recovering the 3D shape of an object from images is one of the fundamental problems in computer vision. It has a variety of applications such as robotics, augmented reality, and human-computer interaction. In recent years, 3D object reconstruction has been greatly enhanced by deep learning. One typical method is to train a neural network that outputs a 3D model directly from an image (Choy et al., 2016; Girdhar et al., 2016; Hane et al., 2017; Fan et al., 2017). Since this method only learns to output plausible shapes from the data, it is difficult to analyze how the method recovers the shape of the object. Recently, several methods of approximating the implicit function by neural networks have been proposed (Mescheder et al., 2019; Park et al., 2019; Chibane et al., 2020; Jiang et al., 2020; Ibing et al., 2021). Since these methods learn the properties of the 3D space, they are more interpretable than methods that estimate the shape directly from an image. However, they do not provide a detailed step-by-step reconstruction process.

While the reconstruction process is an essential perspective in understanding how the model is recovered during inference, it tends to be less noticeable. One possible reason for this is that the 3D model is generally more critical than the reconstruction process since it is sufficient to obtain only the 3D model for many applications. Nevertheless, making the reconstruction process interpretable has some potential. For example, identifying the steps where inference errors occur can feed into the development of better methods. Moreover, analyzing the process of creating a good model may help us to elucidate effective inference methods.

In order to make the reconstruction process interpretable, a 3D object reconstruction method that mimics human modeling using reinforcement learning has been proposed (Lin et al., 2020). When humans use modeling software to create a model, they divide it into two stages: creating a coarse model and refining it. The reinforcement learning method learns an agent for each of these stages. More specifically, starting by placing multiple primitive shapes in 3D space, it learns an agent that predicts a rough shape with primitives and an agent that predicts a detailed shape by deforming the mesh of primitives. As shown in Fig. 1, this method provides an understandable reconstruction process from a series of actions. However,

[a] https://orcid.org/0000-0002-7079-9116
[b] https://orcid.org/0000-0002-5638-2509
[c] https://orcid.org/0000-0002-9165-5912

Ito, S., Ju, B., Kaneko, N. and Sumi, K.
Viewpoint-independent Single-view 3D Object Reconstruction using Reinforcement Learning.
DOI: 10.5220/0010825900003124
In *Proceedings of the 17th International Joint Conference on Computer Vision, Imaging and Computer Graphics Theory and Applications (VISIGRAPP 2022) - Volume 5: VISAPP*, pages 811-819
ISBN: 978-989-758-555-5; ISSN: 2184-4321

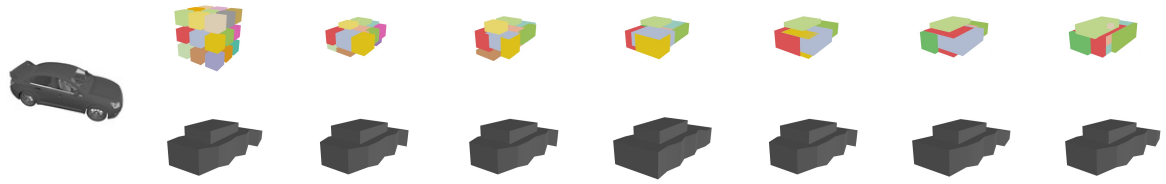

Figure 1: The reconstruction process. The method of (Lin et al., 2020) provides an understandable reconstruction process using the action history. The top row shows the coarse shape reconstruction by deforming the primitives, and the bottom row shows the detailed shape reconstruction by mesh deformation.

training and evaluation were performed using images where all objects are rendered in the same pose and from the same viewpoint. Therefore, the influence of viewpoint changes is unexplored.

In this paper, we propose a 3D object reconstruction method based on reinforcement learning that can handle image input from arbitrary viewpoints. The proposed method is an extension of Lin et al.'s method to handle arbitrary viewpoints. There are two challenges in learning using images from arbitrary viewpoints: 1) how to handle arbitrary viewpoints, and 2) how to train agents efficiently. For the first challenge, we propose a viewpoint-independent image feature extractor network trained on images from a few viewpoints. For the second challenge, we propose a two-stage learning strategy consisting of learning a feature extractor and reinforcement learning. By pre-training a viewpoint-independent image feature extractor network, the proposed method can be trained on single viewpoint images in reinforcement learning. In our experiments, the proposed method achieves better performance than the method of Lin et al. and shows robustness to viewpoints.

2 RELATED WORK

This section reviews 3D object reconstruction from images. We focus on the interpretability of the reconstruction process.

Many methods have been proposed to recover 3D shapes in various representations such as voxels (Choy et al., 2016; Girdhar et al., 2016; Hane et al., 2017; Riegler et al., 2017), point clouds (Fan et al., 2017), and meshes (Wang et al., 2018; Wen et al., 2019). Wang et al. proposed a method to estimate the shape of an object in an input image by transforming an elliptical mesh model as a reference (Wang et al., 2018). This method can interpret the reconstruction process by tracking the model after mesh deformation, but the process takes only a few steps. Recently, approaches based on implicit functions have shown promising results (Mescheder et al., 2019; Park et al., 2019; Chibane et al., 2020; Jiang et al., 2020; Ibing et al., 2021). Implicit functions provide a compact representation of spaces such as surfaces and occupancies. Unlike methods that directly output a model from an image, these methods infer the properties of the space to recover the shape. Therefore, it is possible to analyze how the final shape is obtained. However, this is different from the process of reconstruction from an image.

Another line of work is 3D object reconstruction using a differentiable renderer (Kato et al., 2018; Liu et al., 2019). Differentiable renderers can estimate 3D shapes from images without 3D supervisory data. The 3D models estimated by the network during the learning process can be regarded as a shape reconstruction process. However, it is difficult to obtain an accurate 3D model by inputting a single image only due to the ambiguity of its shape.

Reinforcement learning is a method that allows the interpretation of detailed reconstruction processes even with a single image as input. Lin et al. proposed a two-stage approach for reconstructing the 3D shape of an object from a single image (Lin et al., 2020). It defines the movement of vertices of multiple cuboids as action and learns an agent that roughly approximates the shape of the target object. Subsequently, additional vertices are added to the cuboids. Another agent is then trained to refine the shape. Although this approach is promising in terms of explainability, only images from the single fixed viewpoint are used for training and evaluation. Through preliminary experiments, we found that the accuracy decreased when images from viewpoints unused for training were given. Since reinforcement learning requires a lot of time to obtain good rewards, it is inefficient to train with multiple views. Our method is based on Lin et al.'s method, which is described in detail in the next section.

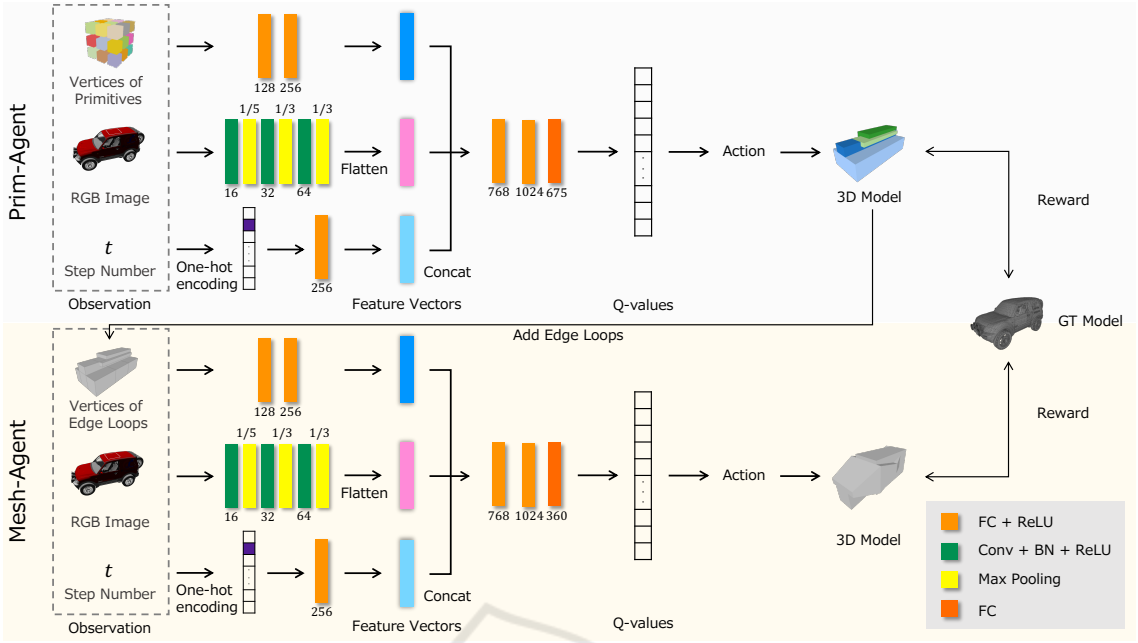

Figure 2: Illustration of the overall framework for 3D object reconstruction based on reinforcement learning. We start by placing multiple primitives in 3D space and learn a Prim-Agent that transforms the vertices of the primitives to roughly approximate the target shape. Subsequently, we add edge loops to the resulting primitives and learn a Mesh-Agent that deforms the mesh to recover the detailed shape. The numbers below the convolution and fully connected layers indicate the output dimension. The numbers above the pooling layers represent the spatial resolution scale.

3 REVIEW OF REINFORCEMENT LEARNING FORMULATION

The proposed method is an extension of Lin et al.'s method (Lin et al., 2020) [1] without viewpoint dependency. This section reviews the formulation of their reinforcement learning method. The overall framework of Lin et al.'s method is illustrated in Fig. 2. In this method, the shape of an object is recovered in two stages in a coarse-to-fine manner. Specifically, it uses the Prim-Agent to fit the 3D shape of the object in the input image with multiple primitives, i.e., cuboids, and the Mesh-Agent to obtain the detailed shape from the model composed of the resulting cuboids. Similar to their method, we also use these agents to reconstruct the 3D shape of an object. The proposed method will be explained in Sec. 4, focusing on the differences from their method.

[1]While the original method takes a depth map as input, it also takes an RGB image as input. The original code is available at https://github.com/clinplayer/3DModelingRL

3.1 Primitive-based Shape Fitting

The goal at the first stage is to fit the rough shape of the object in the input image with several primitives. In this stage, the cuboid is used as a primitive shape. Initially, m^3 cubes are placed evenly on the 3D grid. The shape of the cuboid is defined by the coordinates of the two diagonal vertices. The Prim-Agent manipulates the vertices of a cuboid based on its current state. The environment rewards the Prim-Agent for its actions, and the Prim-Agent is trained to choose the optimal action. The detailed formulation is described below.

State. Let a set of cuboids be $\mathcal{P} = \{P_i\}_{i=1}^{m^3}$. The i-th cuboid P_i is defined by the two vertices $V = (x, y, z)$ and $V' = (x', y', z')$ on the diagonal. The state consists of an input image, a set of cuboids, and a step number. In this stage, m is set to 3.

Action. Moving the vertices of the i-th cuboid P_i can be divided into three types: move V, move V', or delete P_i. The movement range $\mathcal{R} = \{r | r \in [-d, d], r \neq 0\}$ is defined for each axis of each vertex. The action space is a total of $2m^3 \times 2d \times 3 + m^3$ with two vertices of each cuboid, a move in each axis, and

the removal of cuboids. In this stage, $d = 2$ is used, and the total action space is 675.

Reward. In order for the Prim-Agent to choose the appropriate action, the reward function based on the intersection over union (IoU) is designed. The IoU measures the overlap between the two shapes. Let T denote the target shape. The IoU is defined as follows:

$$I_1 = \mathrm{IoU}(\bigcup_i P_i, T), \tag{1}$$

This term captures the global shape. In order for each cuboid to cover much of the target shape, the local IoU is computed:

$$I_2 = \frac{1}{|\bar{\mathcal{P}}|} \sum_{P_i \in \bar{\mathcal{P}}} \mathrm{IoU}(P_i, T), \tag{2}$$

where $\bar{\mathcal{P}}$ is the set of primitives that have not been deleted. These two terms I_1 and I_2 are independent of the number of primitives. To recover the shape of the target with fewer primitives, the reward function at the k-th step is defined as follows:

$$\mathcal{R}_k = \alpha_1(I_1^k - I_1^{k-1}) + \alpha_2(I_2^k - I_2^{k-1}) + \alpha_3(\mathcal{N}^k - \mathcal{N}^{k-1}), \tag{3}$$

where $\mathcal{N}^i$ is the number of deleted primitives at the i-th step and α_1, α_2, and α_3 are weighting coefficients. Here, α_1, α_2, and α_3 are set to 1.0, 0.1, and 0.01, respectively.

3.2 Mesh Deformation

The second stage aims to recover the detailed shape of the object by deforming the resulting mesh of primitives. Edge-based deformation is an effective method to generate a natural shape with a small number of vertices. Lin et al. assign edge loops to the cuboids and train the Mesh-Agent to deform the mesh based on the edge loops.

An edge loop is a series of connected edges on the surface of an object. It circles the object and ends at the starting point. The method of Lin et al. assigns n edge loops to the cuboids obtained in the first stage. For undeleted cuboids, edge loops are generated such that the longest edge is perpendicular to an axis. The number of edge loops assigned to a cuboid is proportional to its volume, and the cuboids with larger volumes are assigned more edge loops. Here, at least two edge loops are assigned to a cuboid.

State. Let $L = \{L_i\}_{i=1}^n$ be the set of edge loops. The i-th edge loop L_i is represented by two diagonal vertices $V_l = (x_l, y_l, z_l)$ and $V_l' = (x_l', y_l', z_l')$. The input image, the set of edge loops, and the number of steps are used for the state. In this stage, n is set to 10.

Action. Similar to Prim-Agent, Mesh-Agent defines its action as the movement of two vertices that make up an edge loop. For Mesh-Agent, $d = 3$ is used, and the total action space is 360.

Reward. The role of the Mesh-Agent is to manipulate the shape obtained by the Prim-Agent in more detail to get closer to the target shape. Therefore, only the IoU difference is used for the reward.

3.3 Imitation Learning

Imitation learning is a method of learning by using actions that are optimal strategies. When the action space is large, the probability of selecting the optimal action by reinforcement learning alone is low, making learning difficult. To solve this problem, Lin et al. proposed a method to generate actions heuristically, namely virtual experts. More specifically, the virtual expert explores all potential actions and selects the action that allows the agent to obtain the maximum reward.

After imitation learning, reinforcement learning is performed while retaining the generated action data. However, if the number of viewpoints of images used for reinforcement learning is increased, a large amount of memory is required to maintain the data.

3.4 Reinforcement Learning

Lin et al. compared several algorithms (Ross et al., 2011; van Hasselt et al., 2016; Hester et al., 2018) and showed that DAgger with virtual experts using double replay buffers based on Double DQN is effective. The core idea is to reuse the experiences gained in imitation learning for reinforcement learning to cope with a large action space. The loss function is determined by a sum of temporal difference update and the supervised loss such that the Q-value of the expert's action is at least marginally higher than the other actions:

$$\mathcal{L}(\theta) = \mathcal{L}_{TD}(\theta) + \mathcal{L}_S(\theta), \tag{4}$$

$$\mathcal{L}_S(\theta) = \max_{a \in A}(Q(s,a;\theta) + l(s,a_E,a)) - Q(s,a_E;\theta), \tag{5}$$

where A is a set of actions, $Q(s,a,\theta)$ is the Q-value of an action a for the state s given the parameters of the network θ, and $l(s,a_E,a)$ is a margin function that is zero when the a is same as the expert's action a_E and positive otherwise.

The reinforcement learning in the proposed method follows the method of Lin et al. except that the parameters of the image feature extraction network are fixed. For more details, please refer to the original paper (Lin et al., 2020).

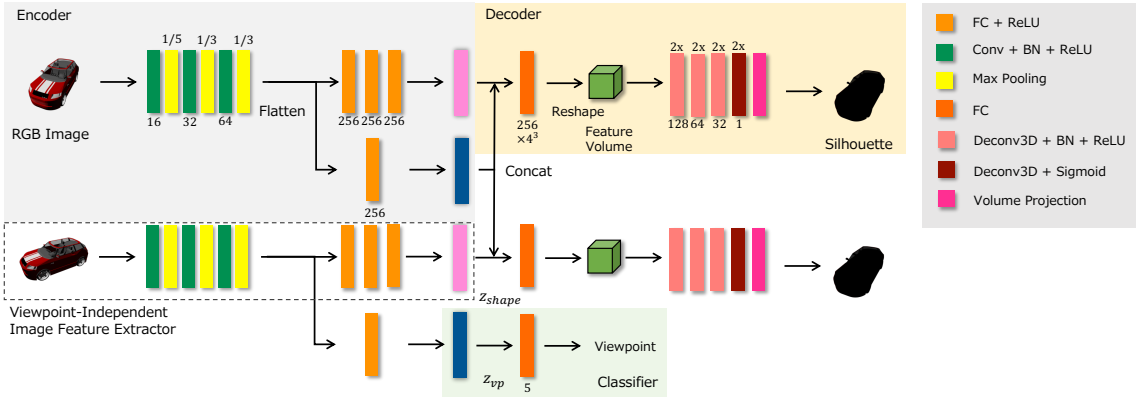

Figure 3: Illustration of the training pipeline for the encoder-decoder network. The encoder takes an RGB image as input and extracts shape features and viewpoint features. The shape and viewpoint features are fed into the decoder network, which outputs a silhouette of the input image corresponding to the viewpoint. By training the network with images from multiple viewpoints and swapping the viewpoint features, the shape and viewpoint features are disentangled. The classification of viewpoints encourages disentangling these features. The encoder-decoder network and the classier are shared between the views. The network that extracts shape features from an image (surrounded by a dashed square) is used in reinforcement learning. The numbers below the convolution and fully connected layers indicate the output dimension. The numbers above the pooling and deconvolution layers represent the spatial resolution scale.

4 VIEWPOINT-INDEPENDENT RECONSTRUCTION

The proposed method eliminates viewpoint dependency by extracting viewpoint-independent features from images. The overall architecture is the same as (Lin et al., 2020), except for the image feature extractor. As shown in Fig. 2, actions are inferred from states, i.e., vertices of models, images, and steps. We train an encoder-decoder network that decomposes image into features that encode object shape and viewpoint. The shape features extracted by this network are used as image features for reinforcement learning.

4.1 Viewpoint-independent Image Feature Extraction Network

The training pipeline for the encoder-decoder network is illustrated in Fig. 3. The encoder network takes an input image I^v of the viewpoint v and outputs the image features. These features are passed through two separate fully connected layers to obtain the shape features z_{shape} and viewpoint features z_{vp}. The decoder network D takes the shape features and the viewpoint features z_{vp} as inputs and produces a 3D occupancy grid. The occupancy grid is then projected onto the predefined viewpoint, yielding a silhouette image I_s. To encourage the learning of the encoder, we use the viewpoint features z_{vp} to classify the viewpoints.

The proposed encoder network is a minor extension of the image feature extractor in the method of Lin et al. The network consists of several convolutional, batch normalization, and max-pooling layers to generate 256-dimensional feature vectors from images. From these feature vectors, shape features are generated through three fully connected layers with the same number of dimensions (i.e., 256). In a similar way, viewpoint features are generated through a fully connected layer, and the resulting features are fed into a classifier consisting of a fully connected layer. The decoder network first constructs 256-dimensional feature volumes of size 4^3 by passing the shape features concatenated with viewpoint features to a fully connected layer and then reshaping it. Then, we upsample the feature volume through three 3D deconvolutional layers while reducing the number of feature channels by half. Finally, we apply a 3D deconvolution to obtain an occupancy map with size 64^3.

Once the proposed network has been trained, the image feature extractor of the proposed network is incorporated into the reinforcement learning framework. While adding the fully connected layers to the original network increases the number of parameters, the image feature extractor does not need to be trained by reinforcement learning. The losses to make this image feature extractor viewpoint-independent are explained in Sec. 4.3.

(a) Input image. From left to right, the viewpoints are 0°, 72°, 144°, 216°, and 288°.

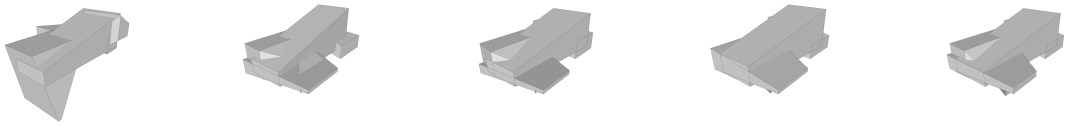

(b) (Lin et al., 2020). From left to right, the IoU values are 0.616, 0.639, 0.657, 0.641, and 0.648.

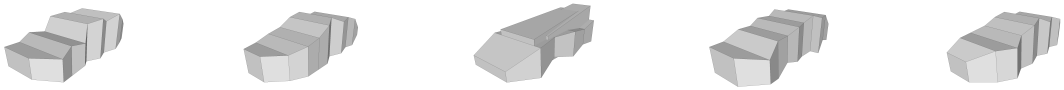

(c) Ours. From left to right, the IoU values are 0.617, 0.702, 0.677, 0.709, and 0.783.

Figure 4: Qualitative comparison of the proposed method with the baseline method. In the baseline method, we trained agents with five different perspectives. The proposed method trained the encoder with five views, but only one view was used for reinforcement learning.

4.2 Volume Projection Layer

The decoder network generates a silhouette image from the occupancy map corresponding to the predefined viewpoint by a projection layer. The proposed method first constructs the occupancy grid to the viewpoint using shape and viewpoint features. For each pixel x, the probability of a silhouette image $I_s(x)$ is then calculated from the occupancies of the voxels through which the ray passes $\{P_i^x\}_{i=1}^N$ as follows:

$$I_s(x) = \max_k P_k^x \tag{6}$$

This means that the maximum occupancy of the voxel where the ray intersects is used as the silhouette value.

4.3 Loss Functions

To train the encoder-decoder network, we use images from different viewpoints $\mathcal{V}$. When each image is passed through the encoder, shape features and viewpoint features are obtained for each. To ensure that the same object has the same shape features, we use the difference in shape features as a loss:

$$\mathcal{L}_{shape} = \sum_{v' \in \bar{\mathcal{V}}} |z^v_{shape} - z^{v'}_{shape}|_1 \tag{7}$$

where $\bar{\mathcal{V}}$ represents all viewpoints except for v. To enforce that the occupancy grid generated from the shape features matches when projected to an arbitrary viewpoint, we compute the silhouette loss:

$$\mathcal{L}_{silhouette} = \sum_{v' \in \mathcal{V}} |\hat{I}_s - D(z^{v'}_{shape}, z^v_{vp})|_1 \tag{8}$$

where $\hat{I}_s$ is the ground truth silhouette image. In addition, we introduce the viewpoint classification loss as an auxiliary loss:

$$\mathcal{L}_{vp} = H(\hat{v}, v) \tag{9}$$

where H is the cross entropy loss and $\hat{v}$ is the ground truth viewpoint. Finally, the overall loss function is defined as follows:

$$\mathcal{L} = \lambda_1 L_{shape} + \lambda_2 L_{silhouette} + \lambda_3 L_{vp} \tag{10}$$

where λ_1, λ_2, and λ_3 are weighting coefficients. Here, λ_1, λ_2, and λ_3 are set to 1.0, 0.5, and 1.0, respectively.

5 EXPERIMENTS

5.1 Experimental Setup

In this work, we focus on the dependency of viewpoints in 3D object reconstruction using reinforcement learning. In this experiment, we basically follow the experimental setup of Lin et al. (Lin et al., 2020) and verify the effectiveness of the proposed method for viewpoint dependency.

Dataset. We use the ShapeNet dataset (Chang et al., 2015) for training and testing. Following Lin et al., we picked up three categories, i.e., cars, airplanes, and guitars from ShapeNet. Each category contains 650 models, where 600 are used for training and the remaining 50 for testing. For all models, we rendered 30 RGB images so that the camera rotated evenly around the object.

Table 1: Comparison of the proposed method with the baseline method. Note that this experiment uses RGB images as input. While Lin et al. only report results using depth images as input, they provide models trained using RGB images. We used the provided models to evaluate Lin et al.'s method that uses a single viewpoint for reinforcement learning.

Method	Viewpoints			Car		Airplane		Guitar	
	Pre-training	RL	Evaluation	Reward	IoU	Reward	IoU	Reward	IoU
Lin et al.	-	1	1	1.014	0.569	0.744	0.200	0.792	0.241
Lin et al.	-	1	5	0.810	0.427	0.590	0.127	0.796	0.297
Lin et al.	-	5	5	0.926	0.517	0.291	0.069	0.914	0.320
Ours	5	1	5	0.961	0.535	0.731	0.204	0.975	0.364
Ours	5	5	5	**0.965**	**0.547**	**0.734**	**0.209**	**0.998**	**0.366**

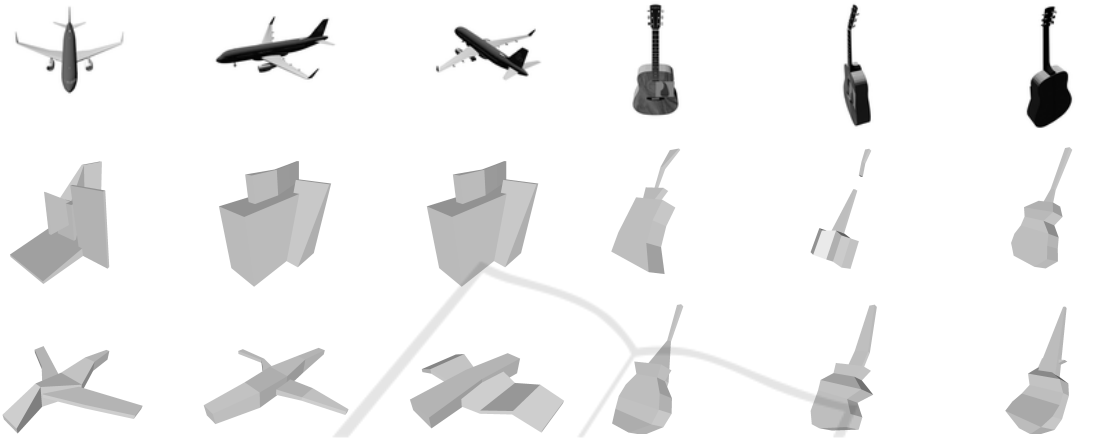

(a) Airplane (b) Guitar

Figure 5: Comparison of the proposed method with the baseline method on the airplane and guitar classes. From top to bottom, input images, results of the baseline method, and results of the proposed method are shown. From left to right, the viewpoints are 0°, 72°, and 144°.

Training. We first train the proposed encoder-decoder network from scratch for 200 epochs. The network was trained using the Adam optimizer (Kingma and Ba, 2015) with a mini-batch size of 32. The initial learning rate is set to $8e$-4. It takes about 2 hours to train the network on an NVIDIA TITAN RTX GPU. Subsequently, the two agents are trained in the same settings as the baseline method (Lin et al., 2020), with 100 epochs each. When training a single viewpoint, it takes about eight days to train two agents. Five viewpoints require five times as much learning time as one viewpoint. Since the reinforcement learning of the proposed method can learn from a single viewpoint, the five-viewpoint setting of the proposed method is only two additional hours to the time required for the one-view setting of the baseline.

5.2 Comparison with the Baseline Method

We compare the proposed method with the baseline method (Lin et al., 2020) using images from five viewpoints, i.e., 0°, 72°, 144°, 216°, and 288°. Here, the reinforcement learning setup in the proposed method is the same as in Lin et al. For the single-view training, we used images from 72°.

Table 1 shows the quantitative evaluation of the proposed method and the baseline method. We use cumulative reward and IoU as evaluation metrics. Since the baseline method trained with only one viewpoint is less accurate than the method trained with five viewpoints, it does not cope with unseen viewpoints. Using multi-view images in the pre-training allows the proposed method to learn with only one viewpoint in the reinforcement learning stage and achieves higher accuracy than the baseline. In addition, the accuracy of the proposed method is further improved when reinforcement learning is performed using images from five viewpoints. However, reinforcement learning with five viewpoints requires a large amount of memory, and the learning speed is slow. On the other hand, the memory needed for pre-training in the proposed method is smaller than reinforcement learning. Moreover, the convergence time of the pre-training and the reinforcement learning using a single

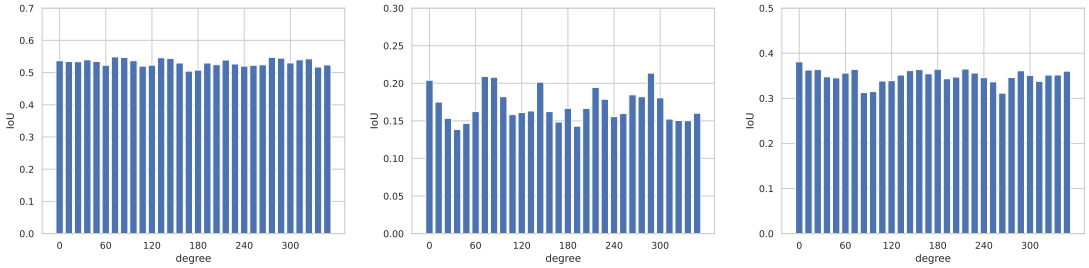

(a) Car (b) Airplane (c) Guitar

Figure 6: Performance of the proposed method with respect to viewpoints.

viewpoint image is shorter than that of the baseline method with five viewpoints, suggesting that the proposed method is more efficient.

The qualitative evaluation of the proposed method and the baseline method is shown in Fig. 4. The proposed method shows qualitatively less shape variation between viewpoints than the baseline method. Fig. 5 shows the results of the proposed method for airplane and guitar classes. As with the car class, similar models are reconstructed from different viewpoints.

5.3 Influence of Viewpoints

The goal of this study is to robustly recover the 3D shape when the input image has a different viewpoint from the training one. Fig. 6 shows mean IoU values of 30 viewpoints. Here, we used a model trained with images from five viewpoints for pre-training and one viewpoint for reinforcement learning. The model trained by the proposed method is almost as accurate as the one used for training, even when images from viewpoints not used for training are input.

Although the proposed method is robust to the viewpoint, the accuracy is low for some shapes as well as the baseline method. Fig. 7 shows the failure example of the proposed method. The proposed method is less accurate for any viewpoint when the shape is complex. Fig. 7(c) shows that the accuracy decreases for viewpoints far from the one used for training, while it increases for viewpoints close to the one used for training.

6 CONCLUSION

In this work, we proposed a 3D object reconstruction method using reinforcement learning that is robust to the viewpoint of the input image. The proposed method first trains an encoder network to decompose image features into geometry and viewpoint factors. Our method fixes the network parameters and

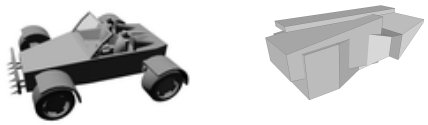

(a) Viewpoint used during training (72°, IoU: 0.408)

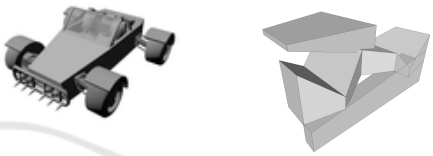

(b) Unseen viewpoint (36°, IoU: 0.218)

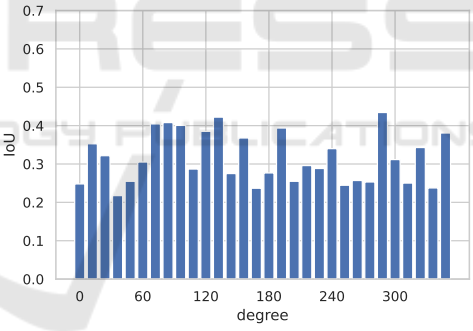

(c) IoU

Figure 7: Failure cases of the proposed method.

uses the network for reinforcement learning as an image feature extractor. The proposed method achieved more accurate estimation results than the baseline method trained on images with multiple viewpoints. In addition, we experimentally show that the proposed method can estimate with the same accuracy even for views that are not used for training.

ACKNOWLEDGEMENT

This work was supported by JSPS KAKENHI Grant Number JP20J13300.

REFERENCES

Chang, A. X., Funkhouser, T. A., Guibas, L. J., Hanrahan, P., Huang, Q., Li, Z., Savarese, S., Savva, M., Song, S., Su, H., Xiao, J., Yi, L., and Yu, F. (2015). ShapeNet: An Information-Rich 3D Model Repository. *CoRR*, arXiv:1512.03012.

Chibane, J., Alldieck, T., and Pons-Moll, G. (2020). Implicit Functions in Feature Space for 3D Shape Reconstruction and Completion. In *IEEE/CVF Conference on Computer Vision and Pattern Recognition (CVPR)*, pages 6968–6979.

Choy, C. B., Xu, D., Gwak, J., Chen, K., and Savarese, S. (2016). 3D-R2N2: A Unified Approach for Single and Multi-view 3D Object Reconstruction. In *European Conference on Computer Vision (ECCV)*, pages 628–644.

Fan, H., Su, H., and Guibas, L. J. (2017). A Point Set Generation Network for 3D Object Reconstruction from a Single Image. In *IEEE Conference on Computer Vision and Pattern Recognition (CVPR)*, pages 2463–2471.

Girdhar, R., Fouhey, D. F., Rodriguez, M., and Gupta, A. (2016). Learning a Predictable and Generative Vector Representation for Objects. In *European Conference on Computer Vision (ECCV)*, pages 484–499.

Hane, C., Tulsiani, S., and Malik, J. (2017). Hierarchical Surface Prediction for 3D Object Reconstruction. In *International Conference on 3D Vision (3DV)*, pages 412–420.

Hester, T., Vecerík, M., Pietquin, O., Lanctot, M., Schaul, T., Piot, B., Horgan, D., Quan, J., Sendonaris, A., Osband, I., Dulac-Arnold, G., Agapiou, J. P., Leibo, J. Z., and Gruslys, A. (2018). Deep Q-learning From Demonstrations. In *Thirty-Second AAAI Conference on Artificial Intelligence (AAAI)*, pages 3223–3230.

Ibing, M., Lim, I., and Kobbelt, L. (2021). 3D Shape Generation With Grid-Based Implicit Functions. In *IEEE Conference on Computer Vision and Pattern Recognition (CVPR)*, pages 13559–13568.

Jiang, C. M., Sud, A., Makadia, A., Huang, J., Nießner, M., and Funkhouser, T. A. (2020). Local Implicit Grid Representations for 3D Scenes. In *IEEE/CVF Conference on Computer Vision and Pattern Recognition (CVPR)*, pages 6000–6009.

Kato, H., Ushiku, Y., and Harada, T. (2018). Neural 3D Mesh Renderer. In *IEEE Conference on Computer Vision and Pattern Recognition (CVPR)*, pages 3907–3916.

Kingma, D. P. and Ba, J. (2015). Adam: A Method for Stochastic Optimization. In *3rd International Conference on Learning Representations (ICLR)*.

Lin, C., Fan, T., Wang, W., and Nießner, M. (2020). Modeling 3D Shapes by Reinforcement Learning. In *European Conference on Computer Vision (ECCV)*, pages 545–561.

Liu, S., Chen, W., Li, T., and Li, H. (2019). Soft Rasterizer: A Differentiable Renderer for Image-Based 3D Reasoning. In *IEEE/CVF International Conference on Computer Vision (ICCV)*, pages 7707–7716.

Mescheder, L. M., Oechsle, M., Niemeyer, M., Nowozin, S., and Geiger, A. (2019). Occupancy Networks: Learning 3D Reconstruction in Function Space. In *IEEE Conference on Computer Vision and Pattern Recognition (CVPR)*, pages 4460–4470.

Park, J. J., Florence, P., Straub, J., Newcombe, R. A., and Lovegrove, S. (2019). DeepSDF: Learning Continuous Signed Distance Functions for Shape Representation. In *IEEE Conference on Computer Vision and Pattern Recognition (CVPR)*, pages 165–174.

Riegler, G., Ulusoy, A. O., and Geiger, A. (2017). OctNet: Learning Deep 3D Representations at High Resolutions. In *IEEE Conference on Computer Vision and Pattern Recognition (CVPR)*, pages 6620–6629.

Ross, S., Gordon, G. J., and Bagnell, D. (2011). A Reduction of Imitation Learning and Structured Prediction to No-Regret Online Learning. In *Fourteenth International Conference on Artificial Intelligence and Statistics (AISTATS)*, volume 15, pages 627–635.

van Hasselt, H., Guez, A., and Silver, D. (2016). Deep Reinforcement Learning with Double Q-Learning. In *Thirtieth AAAI Conference on Artificial Intelligence (AAAI)*, pages 2094–2100.

Wang, N., Zhang, Y., Li, Z., Fu, Y., Liu, W., and Jiang, Y. (2018). Pixel2Mesh: Generating 3D Mesh Models from Single RGB Images. In *European Conference on Computer Vision (ECCV)*, pages 55–71.

Wen, C., Zhang, Y., Li, Z., and Fu, Y. (2019). Pixel2Mesh++: Multi-View 3D Mesh Generation via Deformation. In *IEEE/CVF International Conference on Computer Vision (ICCV)*, pages 1042–1051.